EPS-0486
Submitted to Pa 10 and Pl 1, 3

Determination of the Strong Coupling Constant α_s in Deep Inelastic ep Scattering at HERA

H1 Collaboration

Abstract

The measurement of the strong coupling constant α_s based on jet rates in deep inelastic ep scattering at HERA is discussed. Using the 1994 data with an integrated luminosity of $\approx 3\ \mathrm{pb}^{-1}$ a preliminary determination in next to leading order results in $\alpha_s(M_Z^2) = 0.126 \pm 0.007\,(stat) \pm 0.008\,(sys)$.

1 Introduction

Neutral current deep inelastic electron-proton scattering (DIS) is investigated using data from the 1994 run of the HERA ep collider at DESY. This reaction is denoted as $e(k)\,p(P) \rightarrow e'(k')\,X(h)$, where the symbols in brackets denote the particle four vectors. It is shown in figure 1, which also introduces the basic kinematic quantities used later on.

In 1994 at HERA, electrons of 27.6 GeV momentum are scattered off protons of 820 GeV momentum leading to a center of mass energy of 300 GeV. In the deep inelastic scattering regime, momentum transfers squared $Q^2 > 100$ GeV^2, ($Q^2 = -q^2$) are considered in this analysis. The experiment H1 [1] allows to observe the scattered electron (e') and also the hadronic final state (X), the main interest of the analysis discussed here.

In lowest order, neutral current DIS jet production can be described as purely electromagnetic scattering of the electron off a quark via single photon exchange. In the Q^2 range studied, the exchange of the intermediate vector boson Z° is highly suppressed due to it's large mass. This scattering leads to (1+1) jet events. One jet is caused by the scattered quark (1), the other by the leftover part of the proton (+1), which is only partially observed in the detectors.

Higher jet multiplicities are described in the framework of QCD. The corresponding cross sections are expressed as power series in α_s, such that the leading order (LO) contribution to (2+1) jet events is at $\mathcal{O}(\alpha_s)$. Two generic graphs contribute (see figure 2). As both diagrams contain couplings to gluons it is clear that (2+1) jet production is sensitive to α_s.

The analysis presented in this paper essentially follows the strategy of the pioneering measurement described in [2, 3]. In section 2 the measured jet rates are compared to theoretical predictions and in section 3 the determination of α_s is discussed.

The data presented here were taken with the H1 experiment at HERA in 1994 with an integrated luminosity of ≈ 3 pb^{-1}.

2 Jet rates compared to theoretical predictions

At HERA the fractional (2+1) jet rate is chosen [2] to explore the running of $\alpha_s(\mu^2)$ as function of the varying momentum transfer squared Q^2, which is here taken as the renormalization scale ($Q^2 = \mu^2$).

This method allows to study the evolution of $\alpha_s(Q^2)$ over a wide range of Q^2 by using only one observable in a single experiment. The lowest reachable Q^2 is given by the lower cutoff in Q^2 at which perturbative QCD is considered as an applicable theory, and the upper cutoff in Q^2 is the center of mass energy squared of the collider.

The fractional (2+1) jet rate is defined for each bin in Q^2 as:

$$R_{2+1}(Q^2, y_c) = \frac{\sigma_{2+1}(Q^2, y_c)}{\sigma(Q^2)} \tag{1}$$

Here $\sigma(Q^2)$ represents the sum of (1+1) and (2+1) jet cross sections. The jet resolution parameter y_c is defined as $y_c = m_{ij}^2/W^2$, where m_{ij}^2 is the invariant mass squared of two objects i, j and W is the invariant mass of the hadronic system. This rate is known theoretically in next to leading order (NLO), that means up to $\mathcal{O}(\alpha_s^2)$ [4].

As demanded by the theoretical calculations available in the PROJET [5] and DISJET [6] Monte Carlos, jets are experimentally reconstructed using a modified JADE [7] algorithm with W^2 as the mass scale. This algorithm takes into account the invisible part of the proton remnant, by including a pseudo particle in the clustering procedure representing the missing longitudinal momentum in the event [8]. As the calculation is done for massless partons in NLO it does not perform combinations of massive objects while defining the jets, which makes this Lorentz invariant result as well recombination scheme independent. Therefore the frame of reference in which the experimental jet clustering is performed and the recombination scheme used in the jet algorithm is a free choice of the experiments. In this analysis jet counting is done in the laboratory frame using the JADE recombination scheme, as this combination gives the best correlation of the partonic jet rates and the jet rates obtained at the detector level from reconstructed calorimetric energy deposits [2].

The $\mathcal{O}(\alpha_s^2)$ calculations are only available as Monte Carlos for the calculation of jet cross sections at the parton level and not as event generators. This implies, that the relation between observed jets in the detector and the underlying partonic jet configuration has to be obtained from the available LO event generators. For this purpose LEPTO6.1 [9] is used. Events can be generated using the LO matrix elements alone, referred to as (ME), or by matching leading log parton showers to these matrix elements in order to account for a part of the higher order terms (MEPS).

Figure 3 shows the fractional jet rates, at the level of detector jets compared to MEPS in the phase space regions defined in section 3. The description of the observed jet rates by MEPS is excellent. The jets are required to be measured in the angular region $10° < \vartheta_{jet} < 145°$. All polar angles are calculated with respect to the momentum vector of the incoming proton. Especially the region of small ϑ_{jet} is critical as it contains jets from the initial state parton shower and in addition products from the not well understood proton remnant fragmentation. In this region more jets than predicted by the NLO calculation are observed. Another possibility to avoid the region of phase space where the jet cross section diverges [10] is a cut in the partonic scaling variable z_p $(0 \leq z_p \leq 1)$ defined as

$$z_p = \frac{P \cdot p_{jet}}{P \cdot q} = \frac{1}{2}\left(1 - \cos\vartheta^\star_{jet}\right) \tag{2}$$

Here $\vartheta^\star_{jet}$ denotes the jet scattering angle in the photon parton center of mass system and the region of small z_p corresponds to forward scattering in this Lorentz frame. The ϑ_{jet} and z_p distributions are strongly correlated but account for different tails of the jet phase space. Both are used in this analysis to restrict the (2+1) jet phase space. LEPTO6.1 is used to correct the data to the level of parton jets. These can be compared to the NLO calculation.

3 Determination of α_s

The event selection requires $W^2 > 5000$ GeV^{2}and an electron candidate fulfilling $10° < \vartheta_e < 148°$, and $Q^2 > 100$ GeV^{2}and $y < 0.7$. Here ϑ_e is the angle of the scattered electron, and $y = (P \cdot q)/(P \cdot k)$. W^2 is calculated using the double angle method [11], Q^2 and

$y < 0.7$ are obtained from the electron.

In order to compare the measured jet rates to the NLO calculation it is necessary to apply to the NLO Monte Carlo the same phase space restrictions in terms of electron variables and jet quantities as done in an experimental event selection, otherwise the extrapolation to the full phase space would lead to large uncertainties. The PROJET Monte Carlo was adapted to provide this feature.

Figure 4a shows the measurement of $R_{2+1}(Q^2)$ for a particular set of jet phase space restrictions ($y_c = 0.02$, $10° < \vartheta_{jet} < 145°$, $z_p > 0.10$), corrected to the level of parton jets using MEPS. This is compared to the NLO calculation from PROJET for various $\Lambda_{4,\overline{MS}}$ values assuming that the set MRSH [12] represents the correct parton density parametrizations (PDFs). Only statistical errors are shown. $R_{2+1}(Q^2)$ is translated into three measurements of $\alpha_s(Q^2)$ and fitted to the 2-loop solution of the renormalization group equation. The fit, together with the $\pm 1\sigma$ parameter errors of Minuit [13], is shown in figure 4b. The fitted value for this particular scenario is $\alpha_s(M_Z^2) = 0.126 \pm 0.007\,(stat)$.

To obtain the systematic errors the following procedures are applied.

- **Error on $\alpha_s(M_z^2)$:** The fit is repeated for various other fit scenarios, e.g. changing the ϑ_{jet} cut in the range from 8° to 15°, using $y_c = 0.02$ and 0.03, see table 1 for a full list of systematic errors covered. This automatically takes into account the correlation of the errors between the three bins in Q^2.

  The quoted result is the mean value of these fits $\alpha_s(M_z^2) = 0.126$. The statistical error is the typical statistical error of one scenario (± 0.007). The statistical error ranges from 0.005 - 0.010 depending on the selected phase space. Finally the systematic error is taken as the spread of all fit results (± 0.008) and the total error is the quadratic sum of the statistical and systematic error. The full lines in figure 5 indicate the full range, they correspond to $\alpha_s(M_z^2) = 0.115$ and 0.137.

- **Error on $\alpha_s(Q^2)$:** Each of the scenarios results in measured values of $\alpha_s(Q^2)$ for the three bins in Q^2. At every point the spread of all values is considered to be the systematic error. The points in figure 5 are the results of the fit which gives the mean value of all used scenarios (see above). The inner error bars of these points represent the statistical error of this particular fit and the outer error bar the total error, which is calculated as the quadratic sum of the statistical and systematic error, see table 2. This treats the error as uncorrelated between the points and is an upper estimate of the true error.

The dashed curve in figure 5 is the curve corresponding to the world average of $\alpha_s(M_Z^2) = 0.117$ [14, 15].

One particular point of interest which was investigated in addition to the error sources already discussed in [3] is the correlation of the measured value of α_s in this analysis with the value determined while fitting the PDFs which is then used for evolving the PDFs [2, 18]. This was studied using the GRV94 PDFs which are available for various $\Lambda_{4,\overline{MS}}$ values [16] in the range $0.15 - 0.40$ GeV. Although $\alpha_s(M_Z^2)$ used in the PDFs changes by 0.017, the fitted values only differ by 0.004. This large reduction is due to the fact that the PDF's only depend on α_s via the scaling violations, whereas $R_{2+1}(Q^2)$ is directly proportional to α_s.

Statistics		$\pm\,0.007$
ϑ_{jet} and z_p Cut	0,8,12,15-145;10-140,145,150 (deg) 0.10,0.15,0.20	$\pm\,0.004$
y_c Dependence	0.02,0.03	$\pm\,0.002$
Hadronic Energy Scale	$\pm 5\%$	$\pm\,0.007$
Parton Density Functions	MRSH [12],GRV94 [16],CTEQ-2pM[17]	$\pm\,0.002$
$\Lambda_{4,\overline{MS}}$ used in the PDF's	0.2-0.4 GeV	$\pm\,0.002$
Renormalization and Factorization Scale	$\mu_i^2 = 1/4, 4\,Q^2$ i=f,r	$\pm\,0.003$

Table 1: *The preliminary determination of various sources of systematic errors.*

$\langle Q^2\rangle$ [GeV^2]	$\alpha_s(Q^2)$	stat	sys
210	0.214 $\pm$ 0.046	0.025	0.038
445	0.157 $\pm$ 0.033	0.018	0.028
1400	0.130 $\pm$ 0.034	0.020	0.027

Table 2: *The preliminary values of $\alpha_s(Q^2)$ together with their statistical and systematic errors.*

As an alternative to the QCD model used to correct to the level of partonic jet rates the color dipole model (CDM) [19] was studied. This model does not well describe the jet rates. Moreover the level of disagreement between the CDM and the data varies strongly for the different scenarios. Therefore at this stage only one QCD-model is used for the calculation of the correction factors.

4 Conclusions

Jet rates in neutral current deep inelastic *ep* scattering at HERA are used to extract the strong coupling constant α_s in NLO, leading to a preliminary value of

$$\alpha_s(M_Z^2) = 0.126 \pm 0.007\,(stat) \pm 0.008\,(sys)$$

The measurement is performed following the strategy developed in [2, 3]. This unique measurement allows to study the running of α_s using only one observable at various renormalization scales in a single experiment. The measured value is consistent with the world average.

Acknowledgement We are grateful to the HERA machine group whose outstanding efforts made this experiment possible. We appreciate the immense effort of the engineers and technicians who constructed and maintain the detector. We thank the funding agencies for financial support. We acknowledge the support of the DESY technical staff. We wish to thank the DESY directorate for the support and hospitality extended to the non-DESY members of the Collaboration.

References

[1] H1 Collaboration, (I. Abt, et al.), DESY 93-103, (1993).

[2] R. Nisius, PhD thesis, Aachen preprint PITHA 94/21 (1994).

[3] H1 Collaboration (T. Ahmed, et al.), Phys. Lett. **B346**, 415 (1995).

[4] D. Graudenz, Phys. Lett. **B256**, 518 (1991); D. Graudenz, Phys. Rev. **D49**, 3291 (1994); J.G. Körner, E. Mirkes, G.A. Schuler, Int. J. Mod. Physics **A4**, 1781 (1989); T. Brodkorb, J.G. Körner, Z. Phys. **C54**, 519 (1992).

[5] D. Graudenz, PROJET4.1, CERN-TH.7420/94

[6] T. Brodkorb, E. Mirkes, DISJET manual, Univ. of Wisconsin, MAD/PH/821 (1994); T. Brodkorb, E. Mirkes, Univ. of Wisconsin, MAD/PH/820 (1994).

[7] JADE Collaboration, (W. Bartel, et al.), Z. Phys. **C33**, 23 (1986).

[8] D. Graudenz, N. Magnussen, Proc. Workshop 'Physics at HERA', DESY, Hamburg, Vol. 1, 261 (1991), and contributions therein.

[9] G. Ingelman, "LEPTO 6.1", Proc. Workshop 'Physics at HERA', DESY, Hamburg, Vol. 3, 1366 (1991).

[10] ZEUS Collaboration, (M. Derrick, et al.), DESY-95-016, (1993), accepted by Z. Phys. **C** .

[11] S. Bentvelsen et al., Proc. Workshop 'Physics at HERA', DESY, Hamburg, Vol. 1,23(1991); K.C. Hoeger, ibid., Vol. 1,43.

[12] A.D. Martin, W.J. Stirling, R.G. Roberts, Proc. of the Workshop on Quantum Field theory and Theoretical Aspects of High Energy Physics, eds. B. Geyer and E.M. Ilgenfritz, 11 (1993).

[13] F. James, M. Ross MINUIT program manual.

[14] Particle Data Group, (L. Montanet, et al.), Phys. Rev. **D50**, 1297 (1994).

[15] S. Bethke, Proceedings of the XXXth Rencontres des Moriond 1994, to be published.

[16] A. Vogt, DESY-95-068, (1995).

[17] CTEQ-2pM see Pdflib(1,4,24)

[18] B.R. Webber, Cavendish-HEP-94/15.

[19] L. Lönnblad, ARIADNE4.03, Comput. Phys. Commun. **71**, 15 (1992), and references therein.

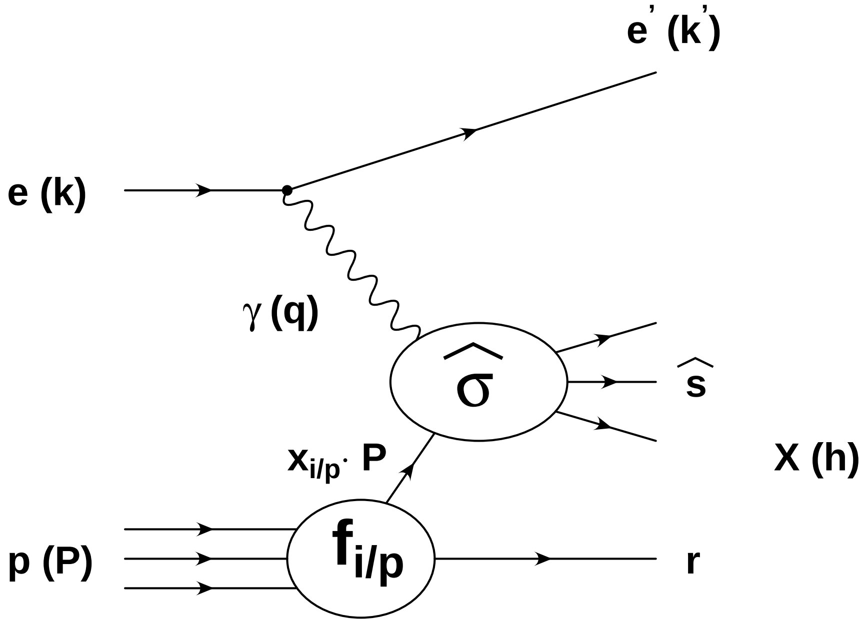

Figure 1: *A sketch of neutral current deep inelastic ep scattering.* $f_{i/p}$ *is the density of partons of sort* i *inside the proton* p *with a fractional momentum* $x_{i/p}$.

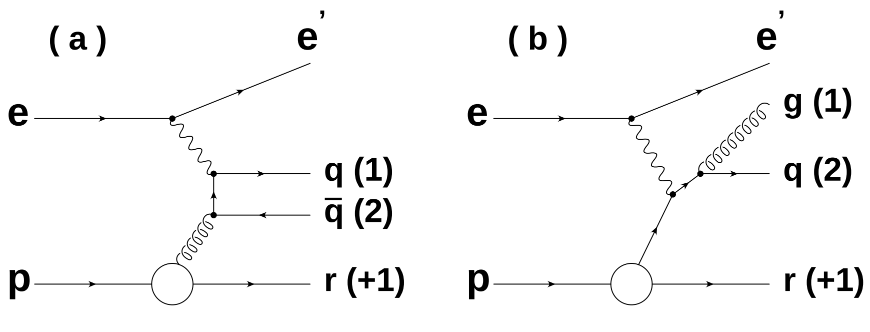

Figure 2: *Generic Feynman diagrams of the LO contributions to (2+1) jet events.*

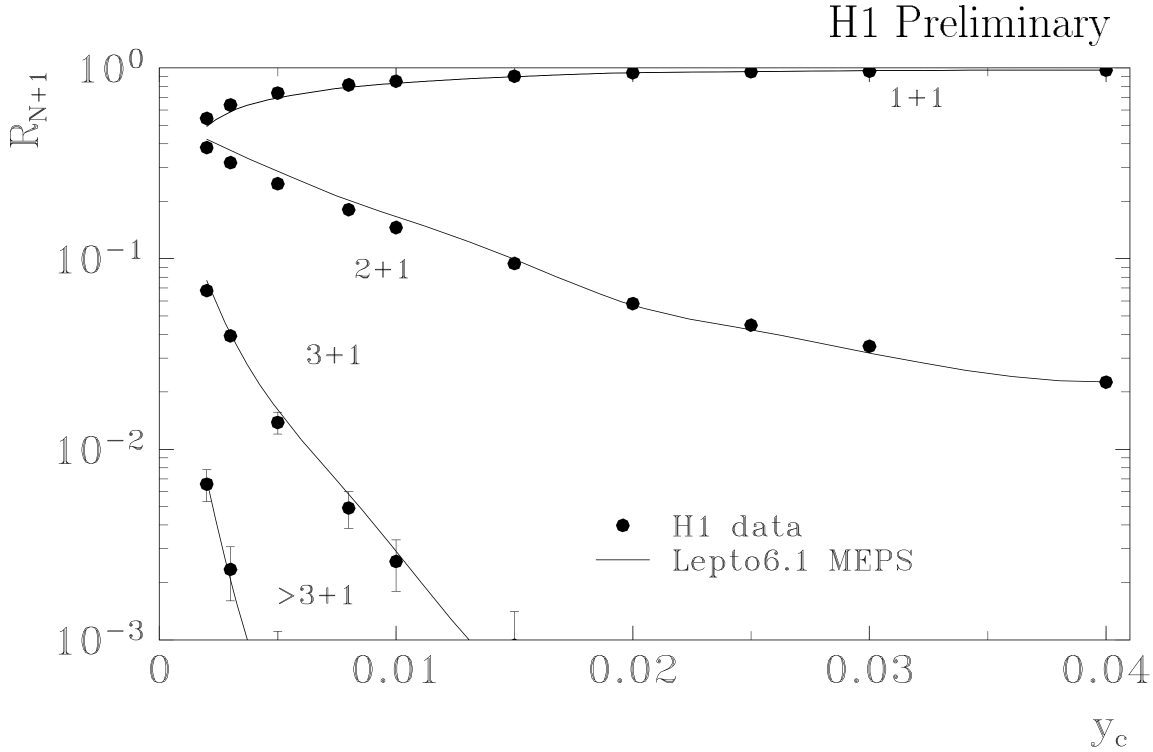

Figure 3: *Fractional jet rates (points) as function of y_c in the kinematic domain $10° < \vartheta_e < 148°$, $Q^2 > 100$ GeV^2, $W^2 > 5000$ GeV^2 and $y < 0.7$. The jets are required to be in the range $10° < \vartheta_{jet} < 145°$ and $z_p > 0.1$ for (2+1) jet events. The uncorrected data is compared to LEPTO6.1 (MEPS) (full lines). Only statistical errors are shown.*

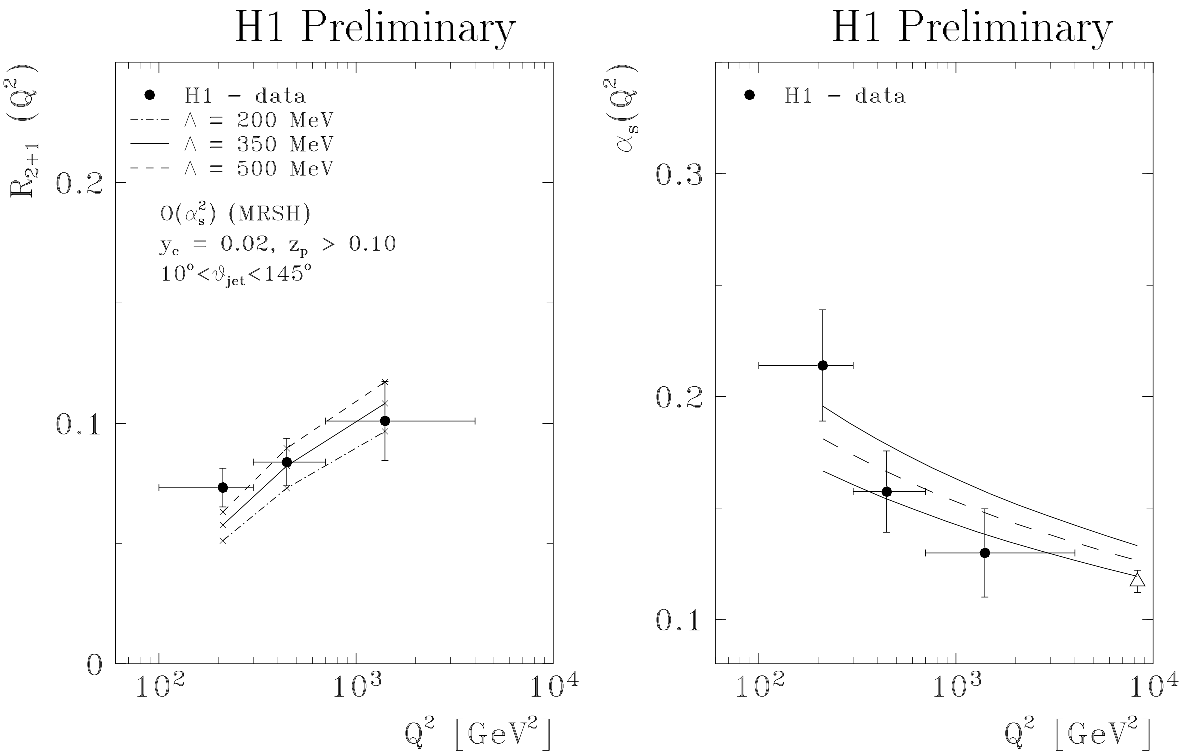

Figure 4: *The α_s measurement for one particular fit scenario $y_c = 0.02$, $10° < \vartheta_{jet} < 145°$, $z_p > 0.1$, using the MRSH parton density parametrizations. The two graphs are plotted both as function of Q^2.*
(a) The corrected jet rate $R_{2+1}(Q^2)$ (points) and the PROJET NLO predictions (lines) for various $\Lambda_{4,\overline{MS}}$ (abbreviated with Λ).
(b) the derived α_s values (points) together with the fit result (dashed line) and the one σ parameter errors (full lines).
Only the statistical errors from the data and the correction factors are shown.
The triangle at $Q^2 = M_Z^2$ indicates the world average $\alpha_s(M_Z^2) = 0.117 \pm 0.005$.

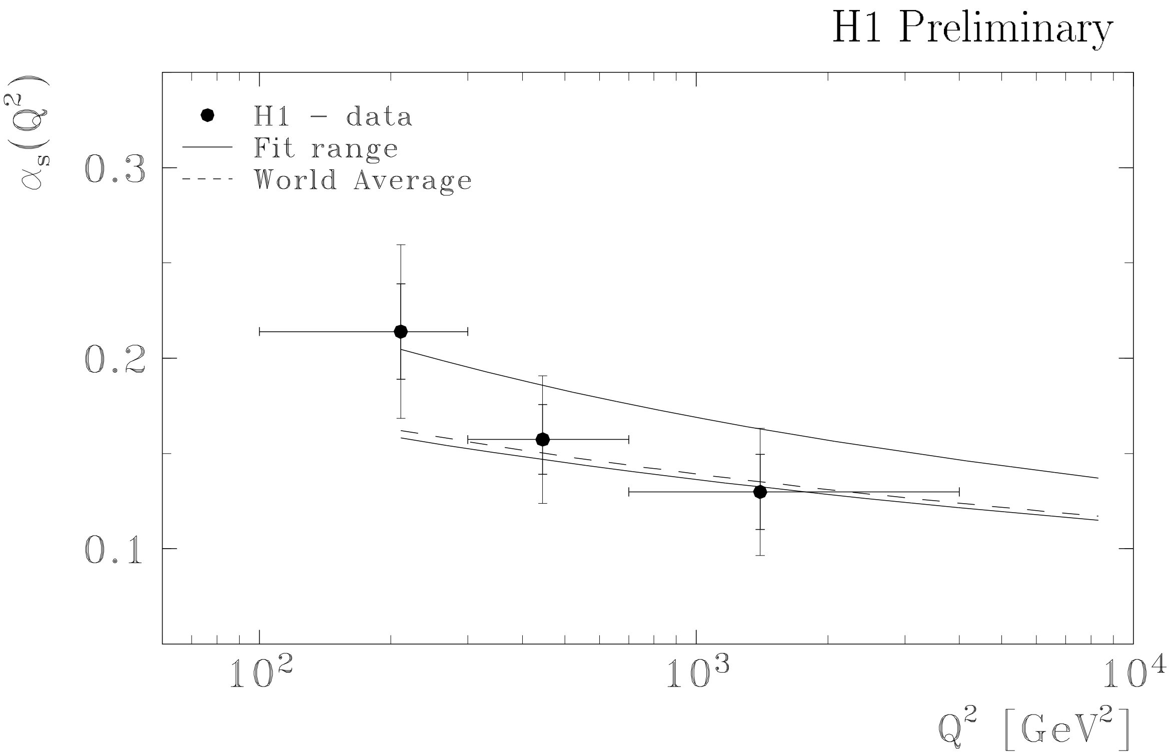

Figure 5: *The α_s measurement from H1 for three bins in Q^2. The data is shown as points with the statistical errors from the data and the correction factors as inner error bars and the total error as full error bars, see table 2 for numbers.*
The dashed line indicates the two loop solution to the renormalization group equation corresponding to $\alpha_s(M_Z^2) = 0.117$, the current world average.
The full lines represent the obtained range for $\alpha_s(M_z^2)$ as measured in this analysis, see text for details.